

D.J. Webb (Referee)

djw@noc.ac.uk

Received and published: 16 April 2016

General Comments

The paper is a study of the effect of one real typhoon and four simulated typhoons on the ocean currents near Green Island. The study region lies in the path of the Kuroshio with depths extending down to 5000m. The study makes use of a finite element model based on the shallow water equations. It reads as a reasonable paper but the description of the model is poor and the paper make a basic error in using a barotropic model for a region of ocean where baroclinic effects are likely to be important.

The paper is not acceptable in its present form. More importantly the use of a barotropic model means that even if other parts of the paper were considerably improved the paper would still not be acceptable for Ocean Science.

Dear Prof. Webb,

Thank you for your useful comments and suggestions on the content and structure of our manuscript. Kuroshio is the potential renewable energy to Taiwan, and Green Island is the potential Kuroshio power plan site. A series of investigation have been conducted to study the hydrodynamics of Kuroshio and Green Island wakes using on board in-situ measurements, X-band Radar, satellite images, and numerical modelling (Hsu, et al., 2014, 2015a, b; Huang, et al., 2014; Liang, et al., 2012, 2013).

Hsu, T.-W., J.-M. Liau, S.-J. Liang*, S.-Y. Tzang and D.-J. Doong, Assessment of Kuroshio current power test site of Green Island, Taiwan, *Journal of Renewable Energy*, 81, 853-863, 2015a.

Hsu, Tai-Wen, Dong-Jiing Doong, Kai-Jiun Hsieh, and Shin-Jye Liang*, Numerical Study of Monsoon-Wake Effect, *Journal of Coastal Research*, 2015b.

Hsu, Tai-Wen, Kai-Jiun Hsieh, and Shin-Jye Liang*, Numerical Analysis of Green Island Wake Due to Passing of Kuroshio, *International Journal of Oceans and Oceanography*, 8(2), 95-111, 2014.

Huang, Shih-Jen, Chung-Ru Ho, Sheng-Lin Lin, and Shin-Jye Liang*, Spatial-Temporal Scales of Green Island Wake Due to Passing of Kuroshio, *International Journal of Remote Sensing*, 35(11-12), 4484-4495, 2014.

Liang, Shin-Jye, Chun-Yi Lin, Tai-Wen Hsu, Chung-Ru Ho*, and Ming-Huei Chang,

Numerical Study of Vortex Characteristics near Green Island, Taiwan, *Journal of Coastal Research*, 29(6), 1436-1444, November, 2013.

Liang, Shin-Jye Liang* and Chiung-Yang Lan, and Ying-Chih Chen, Shallow Water Flow Modeling Using Space-Time Least-Squares Finite-Element Method, *Journal of Marine Science and Technology*, 20(5), 595-602, 2012.

We have modified the manuscript accordingly, and detailed corrections are listed below point by point:

Main points

1. The Shallow Water Equations

1.1 The first paragraph talks about the 'non-conservative' form of the shallow water equations, without stating what is not conserved and why that is better than the normal form which conserves volume and momentum.

→ Governing equations in the conservative (divergence) form contain nonlinear terms such as $\partial(uh)/\partial x + \partial(vh)/\partial y$, where h , u , and v are unknowns and difficult treated using the finite-element approximations. However, these terms can be expressed as $h\partial u/\partial x + u\partial h/\partial x + h\partial v/\partial y + v\partial h/\partial y$ in the non-conservative form, and therefore, can be easily handled by the finite-element approximations. Comparison (advantages and disadvantages) of conservative and non-conservative form can be found in Gunzburger (2012) and Jiang (2013).

Gunzburger, M. D.: *Finite Element Methods for Viscous Incompressible Flows: a Guide to Theory, Practice, and Algorithms*, Elsevier, Singapore, 2012.

Jiang, B.-N.: *The Least-Squares Finite Element Method: Theory and Applications in Computational Fluid Dynamics and Electromagnetics*, Springer Science & Business Media, Berlin, German, 1998.

1.2 The viscosity term in the du/dt and dv/dt equations depends only on the gradient of the velocity fields, not their second order derivative. This is unphysical.

→ Indeed they are typos. Eq. (1) should be

$$\begin{aligned}
& \frac{\partial \eta}{\partial t} + (H + \eta) \frac{\partial u}{\partial x} + u \frac{\partial (H + \eta)}{\partial x} + (H + \eta) \frac{\partial v}{\partial y} + v \frac{\partial (H + \eta)}{\partial y} = 0 \\
& \frac{\partial u}{\partial t} + u \frac{\partial u}{\partial x} + v \frac{\partial u}{\partial y} + g \frac{\partial H}{\partial x} - fv \\
& = -g \frac{\partial z_b}{\partial x} + \frac{1}{h} \left[\tau_x^s - \tau_x^b + \frac{\partial \left(2\rho v_t \frac{\partial (hu)}{\partial x} \right)}{\partial x} + \frac{\partial \left(\rho v_t \left(\frac{\partial (hv)}{\partial x} + \frac{\partial (hu)}{\partial y} \right) \right)}{\partial y} \right] \\
& \frac{\partial v}{\partial t} + u \frac{\partial v}{\partial x} + v \frac{\partial v}{\partial y} + g \frac{\partial H}{\partial y} + fu \\
& = -g \frac{\partial z_b}{\partial y} + \frac{1}{h} \left[\tau_y^s - \tau_y^b + \frac{\partial \left(\rho v_t \left(\frac{\partial (hu)}{\partial y} + \frac{\partial (hv)}{\partial x} \right) \right)}{\partial x} + \frac{\partial \left(2\rho v_t \frac{\partial (hv)}{\partial y} \right)}{\partial y} \right]
\end{aligned} \tag{1}$$

And the viscosity terms does involve the second derivative terms, as usual.

1.3 The equations contain a term which depends on the bottom slope which is not balanced by any other term. This is unphysical.

→ The revised Eq. (1) is a standard shallow-water equations derived from depth averaging the 3D Navier-Stokes equations. The bottom slope, first term of the right hand side of Eq. (1), is balanced by the fourth term of the left hand side of Eq. (1). Refer to Figure 1 for the notation of H , η and h .

1.4 The variables H and Z_b in the equations refer to the same quantity.

→ Relation of the still water depth, $H(x)$, surface elevation, $\eta(x, t)$, and total water depth, $h(x, t)$, is illustrated in the following Figure.

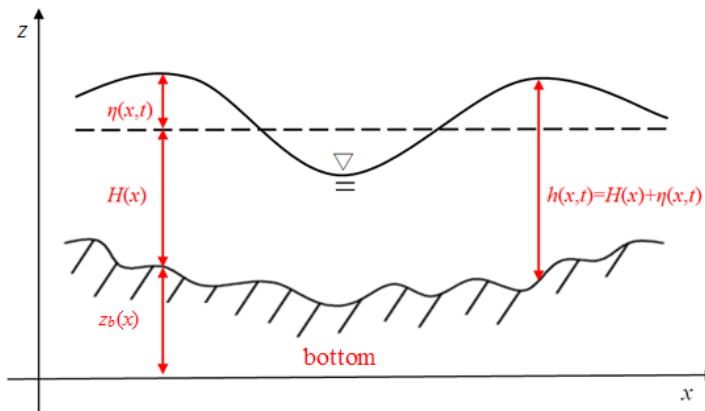


Figure 1. Illustration of still water depth, $H(x)$, surface elevation, $\eta(x, t)$, and total water depth, $h(x, t)$, respectively.

1.5 The term W_g is described as a "gradient of wind speed". It is then defined as having no dimensions and then used as if it is a wind speed.

→ The gradient of wind speed W_g expressed in Eq. (4) involves a scaling parameter B . Powell (1980) suggested that the relationship between the gradient of wind speed W_g and W_{10} can be expressed as $W_{10} = 0.8 W_g$.

2. The Finite Element Method

2.1 The equations involving du/dt and dv/dt in equation (7) do not match the corresponding terms in equation (1).

→ To illustrate the least-squares finite-element method, Eq. (1) is simplified as Eq. (7),

$$\begin{aligned} \frac{\partial \eta}{\partial t} + (H + \eta) \frac{\partial u}{\partial x} + u \frac{\partial (H + \eta)}{\partial x} + (H + \eta) \frac{\partial v}{\partial y} + v \frac{\partial (H + \eta)}{\partial y} &= 0 \\ \frac{\partial u}{\partial t} + u \frac{\partial u}{\partial x} + v \frac{\partial u}{\partial y} - fv &= S_x \\ \frac{\partial v}{\partial t} + u \frac{\partial v}{\partial x} + v \frac{\partial v}{\partial y} + fu &= S_y \end{aligned} \quad (7)$$

where the source terms of the momentum equations are

$$S_x = \frac{1}{h} \left[\tau_x^s - \tau_x^b + \frac{\partial \left(2\rho v_t \frac{\partial (hu)}{\partial x} \right)}{\partial x} + \frac{\partial \left(\rho v_t \left(\frac{\partial (hv)}{\partial x} + \frac{\partial (hu)}{\partial y} \right) \right)}{\partial y} \right] \quad \text{and} \quad S_y = \frac{1}{h} \left[\tau_y^s - \tau_y^b + \frac{\partial \left(\rho v_t \left(\frac{\partial (hu)}{\partial y} + \frac{\partial (hv)}{\partial x} \right) \right)}{\partial x} + \frac{\partial \left(2\rho v_t \frac{\partial (hv)}{\partial y} \right)}{\partial y} \right]$$

The Newton method is applied to linearize the nonlinear terms in Eq. (7), and the resulting equations are

$$\begin{aligned} \frac{\partial \eta}{\partial t} + H \frac{\partial u}{\partial x} + u \frac{\partial H}{\partial x} + \frac{\partial (\tilde{\eta}u + \eta\tilde{u} - \tilde{\eta}\tilde{u})}{\partial x} + H \frac{\partial v}{\partial y} + v \frac{\partial H}{\partial y} + \frac{\partial (\tilde{\eta}v + \eta\tilde{v} - \tilde{\eta}\tilde{v})}{\partial y} &= 0 \\ \frac{\partial u}{\partial t} + \left(\tilde{u} \frac{\partial u}{\partial x} + u \frac{\partial \tilde{u}}{\partial x} - \tilde{u} \frac{\partial \tilde{u}}{\partial x} \right) + \left(\tilde{v} \frac{\partial u}{\partial y} + v \frac{\partial \tilde{u}}{\partial y} - \tilde{v} \frac{\partial \tilde{u}}{\partial y} \right) - fv &= S_x \\ \frac{\partial v}{\partial t} + \left(\tilde{u} \frac{\partial v}{\partial x} + u \frac{\partial \tilde{v}}{\partial x} - \tilde{u} \frac{\partial \tilde{v}}{\partial x} \right) + \left(\tilde{v} \frac{\partial v}{\partial y} + v \frac{\partial \tilde{v}}{\partial y} - \tilde{v} \frac{\partial \tilde{v}}{\partial y} \right) + fu &= S_y \end{aligned} \quad (8)$$

2.2 The model (equations 7) appears to have no Coriolis term. This is unphysical. It also has the unphysical bottom slope terms.

→ The revised Eq. (7) includes the Coriolis terms. Effect of Coriolis force on the hydrodynamics of Kuroshio and downstream Green Island wakes has been investigated (Huang, et al., 2014) and found insignificant for the study domain (80 km x 66 km) considered.

2.2 In equation (9) the definition of the variables is not explicit enough. Are they point values or terms in a local polynomial expansion within each grid cell. Are the grids or points the same for all three sets of variables?

→ Unknowns $\underline{u} = \{\eta, u, v\}^T$ are approximated by the space-time polynomial interpolations $M(x, y)$ and $N(t)$ over the space-time element. $M(x, y)$ and $N(t)$ are the local polynomial expansion within each element. The Unknowns $\underline{u} = \{\eta, u, v\}^T$ are defined using the same nodes (grids/points).

2.3 What is the definition of the functions $M(x, y)$?

→ Depending on the type of elements used, $M(x, y)$ and $N(t)$ can be linear or high order polynomials. In this study, as the computational meshes illustrated in Figure 1b, 3-node triangular meshes in space and continuous linear meshes in time are employed.

2.4 At this stage the residuals R have not been defined so substituting (9) into (8) does not result in equation (10).

→ Substituting the approximations, Eq. (9) into Eq. (8), resulting Eq. (10)

$$\begin{aligned} \begin{Bmatrix} R_\eta^e \\ R_u^e \\ R_v^e \end{Bmatrix} &= \begin{bmatrix} MN_2' + (\tilde{u}_x + \tilde{v}_y)MN_2 & (HM_x + H_xM + \tilde{\eta}M)N_2 & (HM_y + H_yM + \tilde{\eta}M)N_2 \\ 0 & MN_2' + (\tilde{u}M_x + \tilde{u}_xM + \tilde{v}M_y)N_2 & (\tilde{u}_yM - fM)N_2 \\ 0 & (\tilde{v}_xM + fM)N_2 & MN_2' + (\tilde{u}M_x + \tilde{v}M_y + \tilde{v}_yM)N_2 \end{bmatrix} \begin{Bmatrix} \eta \\ u \\ v \end{Bmatrix}^{n+1} \\ &+ \begin{bmatrix} MN_1' + (\tilde{u}_x + \tilde{v}_y)MN_1 & (HM_x + H_xM + \tilde{\eta}M)N_1 & (HM_y + H_yM + \tilde{\eta}M)N_1 \\ 0 & MN_1' + (\tilde{u}M_x + \tilde{u}_xM + \tilde{v}M_y)N_1 & (\tilde{u}_yM - fM)N_1 \\ 0 & (\tilde{v}_xM + fM)N_1 & MN_1' + (\tilde{u}M_x + \tilde{v}M_y + \tilde{v}_yM)N_1 \end{bmatrix} \begin{Bmatrix} \eta \\ u \\ v \end{Bmatrix}^n + \begin{Bmatrix} \tilde{S}_\eta \\ \tilde{S}_u \\ \tilde{S}_v \end{Bmatrix} \end{aligned} \quad (10)$$

2.5 The paper does not explain what boundary conditions were used or how they were introduced into the finite element equations.

→ The boundary conditions are introduced from Line 11 to Line 19 of Page 10:

The flow field data of HYCOM (HYbrid Coordinate Ocean Model) on 7 November 2014 after interpolation to the model grids, shown in Fig. 2a, is utilized to initiate the model. The choice of this particular flow field as the initial condition is based on the hypothesis proposed by Zheng and Zheng (2014) in which the downstream Green island wake is prone to occur when Kuroshio mainstream heads on the island. Figure 2b shows the boundaries of the study domain. AB is the land boundary where no flux and free-

slip boundary condition is applied, BC is the open boundary where the radiation boundary conditions is specified, and CD, DO, and OA are the velocity boundaries using the flow field data from HYCOM on 7 November 2014.

3. Use of the model

3.1 The Kuroshio is a strong baroclinic ocean current. The region of research includes large regions of stratified ocean. As a result the ocean's response to any forcing is expected to contain both baroclinic and barotropic components.

→ Baroclinic effect could be important for the problem considered. However, the 2D shallow-water model is our first step to study the hydrodynamics of Kuroshio and downstream Green Island wakes. We have been working on the development of a sigma coordinate multi-layer shallow-water model which both baroclinic and barotropic components are considered. Hopefully, application of the multi-layer shallow-water model could provide the detailed 3D flow structures in the near future.

3.2 The model used is purely barotropic. In addition in a region where the strong baroclinic Kuroshio extends to much deeper levels the model depth field is limited to 360 m.

→ The 2D shallow-water model is a simple and purely barotropic model. However, Kuroshio is a sub-surface flow where flow mainly occurs at the top 400 m layer of water with an average current speed around 1.0 m/s; Water below 800 m is essentially motionless (Chang et al., 2013). Our study mainly focuses on the region around Green Island where water depth ranges from 5 m to 2000 m, most area of interest with water depth about 500 m.

3.3 The bottom friction terms appear to be used, with the assumption of a solid bottom and a water depth of 360 m, even when the water depth is far in excess of 360 m.

→ Bottom friction could be important, especially for the shallow water area. One objective of the study is to identify the envelope of the meandering vortex streets of Green Island wake, as illustrated by the figure below. These regions are not suitable for installation, maintenance, and operation of the submerged turbines for the current energy. The water depth within the envelope of the meandering vortex streets ranges from 50m to 2000 m. Kuroshio mainly occurs at the top 400 m layer of water, and turbines are submerged in water depth of 50 m to 200 m. So we limit the water depth within 360 m and find the bottom frictions are insignificant to the downstream Green Island wake (Hsu, et al., 2014; 2015a).

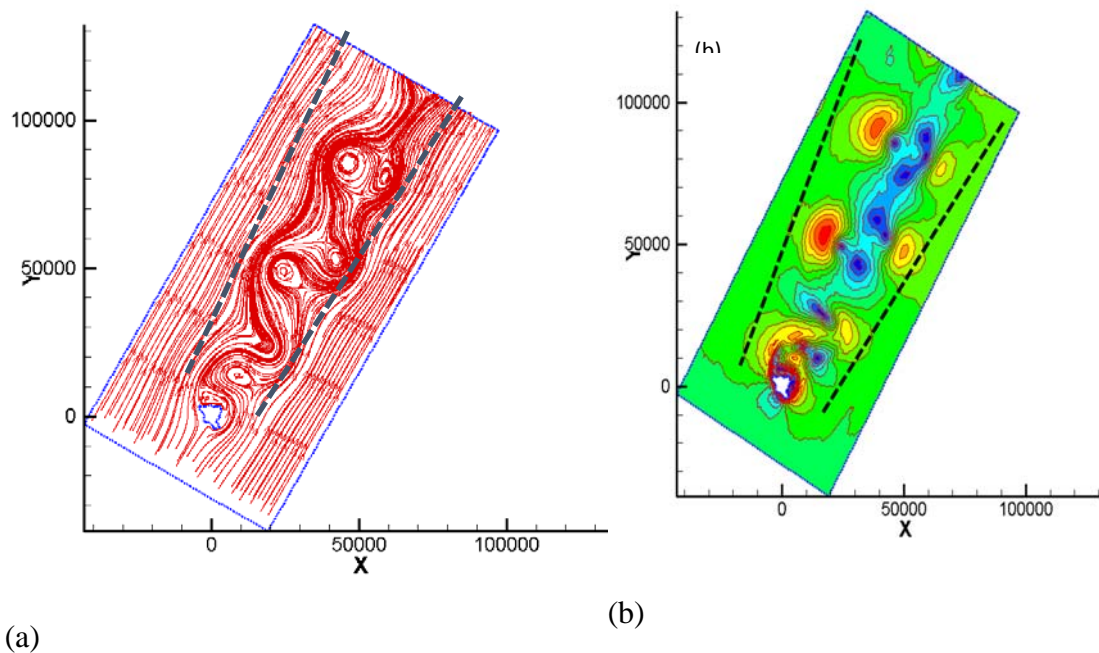


Figure 2: Envelope of the meandering vortex streets of Green Island wake: (a) streamlines and (b) current speed contours in m/s from SWEs model.

3.4 According to figure 1, the ridge between Green Island and Taiwan has depths of between 250 m and 500 m. It is just possible that the flow across the ridge is predominantly barotropic so that locally a barotropic model may be acceptable. This needs to be demonstrated. However even if demonstrated it is very unlikely that a barotropic model will give satisfactory results over the whole domain.

→ We have systematically study the hydrodynamics of Kuroshio and Green Island wakes around the southeastern Taiwan and Green Island. Computed results have been compared favorable with the in-situ measurement, satellite images, X-band radar, and POM modelling (Hsu, et al., 2015a). Salient features of the downstream island wakes are well reproduced. Temporal and spatial scale of the downstream island wakes are also reasonable. Apparently, the barotropic shallow-water model is able to reproduce salient features of the meandering downstream island wakes. This might attribute to the sub-surface flow characteristic of Kuroshio. As addressed in the previous, we have been working on the development of the multi-layer shallow-water model, and hope it could provide the detailed 3D flow structures in the near future.

4. Figures

4.1 Figures 1, 5, 6 to 8 and 10 to 16 were much too small.

→ The original figures are larger and clearer.

4.2 Figure 1. Green island appears to be much further from the coast of Taiwan in (b) than it does in (a).

→ Shape and location of Green Island of Figure 1 (a) and (b) are very close, though not identical, because they are from different maps and resolutions. The difference of the two are smaller than an element size, i.e. smaller than 250 m.

4.3 Figure 2. This shows stream lines not contours of flow speed.

→ Thank you for the corrections. You are right. Figure 2 plots the streamlines, not flow speed, from HYCOM.